Original Article

3D-printed cranial models simulating operative field depth for microvascular training in neurosurgery

Vadim Byvaltsev[1], Roman Polkin[1], Dmitry Bereznyak[1], Morgan B. Giers[2], Phillip A. Hernandez[2], Valery Shepelev[1], Marat Aliyev[1]

[1]Department of Neurosurgery and Innovative Medicine, Irkutsk State Medical University, Irkutsk, Russia, [2]School of Chemical, Biological, and Environmental Engineering, Oregon State University, Corvallis, Oregon, United States.

E-mail: *Vadim Byvaltsev - byval75vadim@yandex.ru; Roman Polkin - roman.polkin@gmail.com; Dmitry Bereznyak - barbarishd@gmail.com; Morgan B. Giers - morgan.giers@oregonstate.edu; Phillip A. Hernandez - hernandp@oregonstate.edu; Valery Shepelev - shepelev.dok@mail.ru; Marat Aliyev - a.marat.a0903@mail.ru

*Corresponding author:
Vadim Byvaltsev,
Department of Neurosurgery and Innovative Medicine,
Irkutsk State Medical University, Irkutsk, Russia.

byval75vadim@yandex.ru.

ABSTRACT

Background: The skills required for neurosurgical operations using microsurgical techniques in a deep operating field are difficult to master in the operating room without risk to patients. Although there are many microsurgical training models, most do not use a skull model to simulate a deep field. To solve this problem, 3D models were created to provide increased training in the laboratory before the operating room, improving patient safety.

Methods: A patient's head was scanned using computed tomography. The data were reconstructed and converted into a standard 3D printing file. The skull was printed with several openings to simulate common surgical approaches. These models were then used to create a deep operating field while practicing on a chicken thigh (femoral artery anastomosis) and on a rat (abdominal aortic anastomosis).

Results: The advantages of practicing with the 3D printed models were clearly demonstrated by our trainees, including appropriate hand position on the skull, becoming comfortable with the depth of the anastomosis, and simulating proper skull angle and rigid fixation. One limitation is the absence of intracranial structures, which is being explored in future work.

Conclusion: This neurosurgical model can improve microsurgery training by recapitulating the depth of a real operating field. Improved training can lead to increased accuracy and efficiency of surgical procedures, thereby minimizing the risk to patients.

Keywords: 3D printing, Cranial approach, Microsurgery, Microvascular training, Neurosurgery, Skull model

INTRODUCTION

The treatment of cerebrovascular diseases often requires complex microsurgical techniques. Depending on the location, surgery can be performed in a superficial or deep operative field. Diseases requiring deep field operations include:

- Cavernous malformations in the cerebral peduncles,[8] midbrain,[17] pons,[46] and other cavernomas of the brainstem[23]
- Arteriovenous malformations in the basal ganglia, thalamus,[27] choroid plexus,[13] brain stem,[18] and cerebellum[43]

- Complex aneurysms of the anterior inferior cerebellar artery,[24] posterior inferior cerebellar artery,[41] basilar artery,[26] and middle cerebral artery[20]
- Skull base tumors.[32,42]

Surgical treatments of the conditions above are performed using various operative approaches and require a surgeon to maneuver in a deep operative field with fine structures using specialized surgical equipment to ensure accurate movements. In recent decades, the surgical training model has modernized with two new concepts: the objective assessment of surgical skill and the development of operating techniques in the laboratory.[33,35] Mastering neurosurgical skills in the laboratory transfer the microsurgical learning curve from patient to laboratory, which in turn improves patient safety and minimizes risk.[3,6,19] Special tools are required for the various microsurgical training available in the laboratory, including microsurgical instruments, a stereoscopic microscope, USP 8-0 or thinner suture material, and blood vessels or vessel models.[4,10] Plastic tubes,[2] chicken brachial arteries,[11,21] turkey wings,[16] human cadaveric material,[39,45] and rat arteries[29] have been used to simulate human blood vessels. A large number of comparative studies have been conducted to determine the advantages and disadvantages of each type of training.[1,7,14,30,44] The main drawback of these training models is that they do not recapitulate the human skull. In this regard, such models do not include a realistic depth of the operational wound and precise modeling of the angle of attack. In addition, there are none that simulate the unstable position of the hands-on different parts of the skull. Technological developments, such as 3D computed tomography (CT) and 3D printing, now allow for the creation of replicated human skulls.[9,37] In this study, 3D printed models of the human skull were used as training models for commonly used neurosurgical approaches. These models allow trainees to develop their deep field microsurgery skills using different approaches and different hand positions on the human skull. Utilizing this affordable model, young surgeons will be able to practice deep anastomoses under real operating room conditions.

MATERIALS AND METHODS

Creation of the 3D skull training model

Scanning

A Siemens SOMATOM Force CT Scanner was used for imaging the patient's head [Figure 1]. All participants provided written informed consent before enrolment in the study.

Segmentation

The CT data were exported as a DICOM file and converted to a stereolithography (STL) file using Mimics 17.0 (Materialize NV, Belgium). The CT provided high-resolution images of the human skull and all relevant anatomical features. Bone tissue was segmented by thresholding. Thresholding gave an imperfect segmentation, including unrealistic holes or excess structures. Small portions of the STL were corrected by hand to remove noisy structures and draw missing features to ensure the STL are not damaged and can be printed.

Approach selection and slice

Using Autodesk 3Ds Max (Autodesk, USA), a hole can be created in the digital skull model. The neurosurgical approach being simulated will depend on the location and size of the hole. Autodesk 3Ds Max was also used to crop the skull STL at specific angles. The cropped side of the skull provided a stable surface for the 3D printed model to rest on, simulating a rigid head fixation system. The angle of the cropping also simulated different head positions during surgery.

Surface reconstruction

Compact and spongy bone are difficult to distinguish when using a single threshold value. This can lead to the formation of small holes on the skull surface. Holes can be reconstructed with Geomagic Studio 13.0 (3D Systems, USA). The number and distribution of polygon elements in the STL mesh will affect the surface quality of the printed model. Due to the various transformations and conversions that result from the scan and postprocessing, the mesh density might be very high in certain regions of the STL. The mesh density impacts printing time and model resolution, so optimizing mesh density is important. The tools in Geomagic's "polygons" menu can automate the refinement of the mesh.

Polish

The data were then exported as an OBJ file and loaded into Autodesk Mudbox (2012) (Autodesk, USA), where the model structures are smoothed.

Final inspection

The OBJ file may have small errors and should be carefully checked using Autodesk Meshmixer (Autodesk, USA) before printing.

Printing

A 3D printer with fused deposition modeling technology printed the model using white polylactic acid materials. The printing process took 26 h.

Assessment of the 3D skull training model

Two operations were used to assess the 3D skull training models: an end-to-end microanastomosis on the chicken
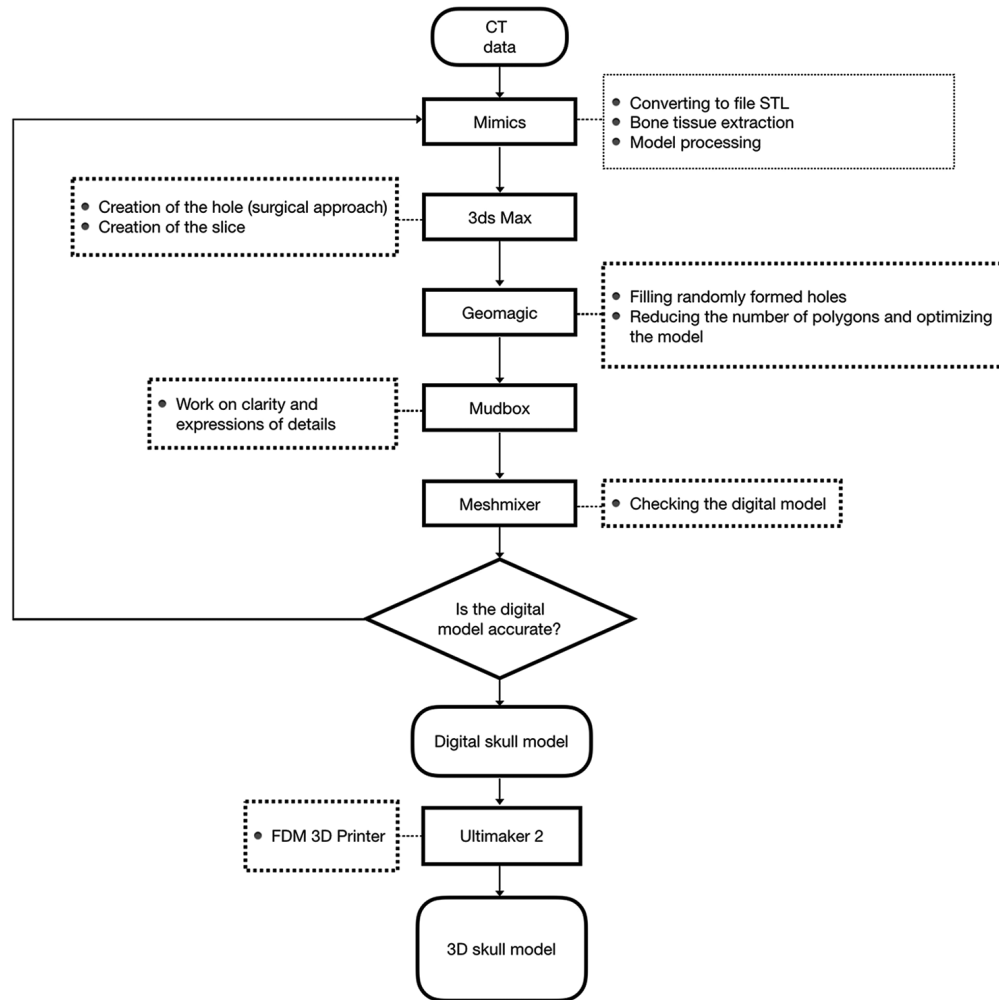
Figure 1: Model-making process.

femoral artery using a lateral supraorbital approach and an end-to-end microanastomosis on the rat abdominal aorta using a retrosigmoid approach. The cranial approach models were evaluated by two expert neurosurgeons experienced in performing surgery in the deep operating field. They subjectively assessed the face validity, as well as the convenience of using three-dimensional models in laboratory training.

Using the 3D skull training model: a lateral supraorbital approach

Chicken thighs purchased from a grocery store were used.

Preparation

Microsurgical scissors, forceps, needle holders, USP 8-0 suture material, microvascular clips, and approximators were collected and are required for the operation.

Approach

A skin incision was made parallel to the femoral bone. The femoral muscles were then separated from the femoral bone to expose the artery, vein, and nerve [Figure 2].

Microdissection

The thigh was placed in a neurosurgical model under an operating microscope [Figure 7a-d]. The femoral artery was microdissected away from the underlying tissue. During isolation, the arterial branches were ligated to ensure mobility. A green latex rectangle was placed under the femoral artery for better visualization. An approximator was placed on the selected vessel leading to where the femoral artery intersects. The ends of the vessels were washed with saline solution to remove clots. Remains of the adventitia were removed from the ends of the vessel.
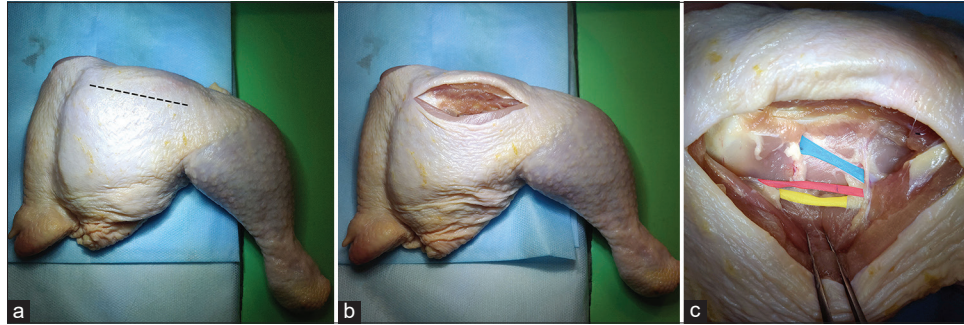
Figure 2: Incision site on the chicken thigh for subsequent work in the deep operative field. (a) The contour of the incision is parallel to the femur, (b) The incision is performed; the muscles are separated from the femur, (c) The anatomy of a chicken thigh (a vein is highlighted blue, an artery is highlighted red, a nerve is highlighted yellow).

Suture

A microanastomosis was performed using the end-to-end technique. The first stay sutures were placed at the 9 and 3 O'clock positions. Three sutures were then placed on both the front and back walls of the vessel. Additional sutures may be placed if necessary.

Patency test

After the microanastomosis, an insulin syringe was inserted into the proximal area of the vessel through which physiological saline was injected to test patency and tightness of the suture.

Using the 3D skull training model: a retrosigmoid approach

Wistar rats were used. All animal housing and experiments were conducted in strict accordance with the institutional Guidelines for Care and Use of Laboratory Animals.[12]

Preparation

The operation required microsurgical scissors, forceps, a needle holder, spring retractors, USP 8-0 suture material, microvascular clips, and approximators. The operation was performed under general anesthesia with an intramuscular injection of ketamine (100 mg/kg) and xylazine (10 mg/kg). After the rat was anesthetized, it was stabilized in the prone position on a pad. The rat was shaved on and around the skin incision.

Approach

The skin incision was made from the xiphoid process to the pubic symphysis along the midline. The abdominal fascia and abdominal muscles were cut along the linea alba and a laparotomy was performed.

Macrodissection

The use of retractors allowed the abdominal wall to be opened so that the abdominal organs were completely exposed. The organs were then moved to the right side of the abdominal wall and covered with gauze soaked in saline to minimize fluid loss. Blunt dissection of the retroperitoneal fat was performed with cotton swabs, effectively exposing the aorta, smaller arterial branches, and the adjacent inferior vena cava.

Skull placement, microscope preparation, and microdissection

It is vital that the operative field and vessels are kept moist throughout the procedure. This prevents the vessels from drying out and becoming more fragile. Dissection of the abdominal aorta from the adjacent vena cava required high magnification with a surgical microscope. At this stage, the skull model and operating microscope are utilized. A pad with a body cutout was placed on top of the rat to position the skull on a flat surface. The chosen neurosurgical model is then placed and the entire structure is positioned under the operating microscope [Figure 3]. The abdominal aorta and the inferior vena cava are covered by the connective and fat tissue which is removed using an acute dissection. During isolation, the arterial branches were ligated to ensure mobility.

Suture

A green latex rectangle was placed under the aorta for better visualization. An approximator was placed on the selected vessel leading to the aortic intersection. The ends of the vessels were washed with saline solution to remove clots. The first stay sutures are applied at the 9 and 3 O'clock positions. Three sutures are then placed on the front and back walls of the vessel. Additional sutures may be placed if necessary.

Hemostasis

After completion of the anastomosis, the suture line was covered with a hemostatic sponge. The distal clip of the approximator was opened first. After 1–2 min, the proximal clip of the approximator is opened to aggregate platelets and seals the suture line. The anastomosis was observed for 5 min before the hemostatic sponge was removed.

Euthanasia

After the operation, the rats were euthanized with CO_2 gas and cervical dislocation was performed in accordance with standard protocols.
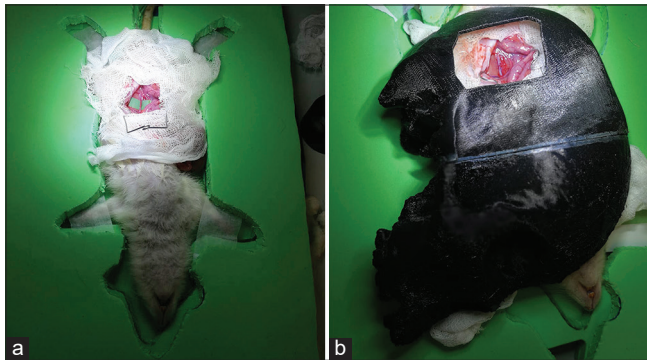

Figure 3: Model use for rat anastomosis. (a) Pad placement, (b) placement of a skull model.

RESULTS

The face validity and the ability to incorporate the printed model into current microneurosurgical training programs were positively noted by expert neurosurgeons.

The ability to use a variety of approaches allows for diverse surgical training. The skull models can simulate 5 operative approaches and provide varying distances to the operation target [Figure 4]. The complexity of the operative technique changes depending on the depth [Table 1].

A "hand contact" technique [Figure 5], where fingers act as support, is used to stabilize the position of the instruments and reduce tension. Based on the type of surgical intervention performed, the support can be carried out with the hypothenar eminence, the fingertips, or the little finger. For more complex training, no support should be used so that the hands can experience maximum tension.

All models have a flat base to ensure stability on the benchtop. The angle of the slice determines the positioning of the skull and the trepanation window located on it, simulating the operating position of the patient and a head secured in a rigid fixation system [Figure 6]. The trepanation window corresponds anatomically to cranial landmarks. The angle of attack depends on the approach, incision, distance to the operation target, position of the hands, and type of surgery.

Figure 4: 3D skull models. (a) Retrosigmoid approach, (b) frontal interhemispheric approach, (c) expanded parietal interhemispheric approach, (d) occipital interhemispheric approach, (e) lateral supraorbital approach.
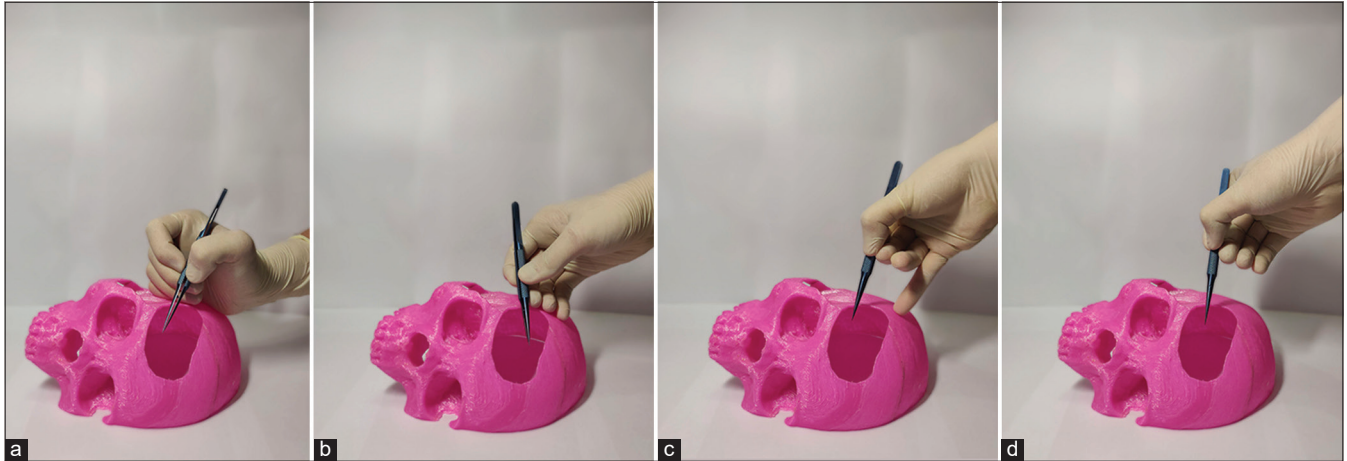
Figure 5: "Hand contact" technique with different methods of positioning the hand on the surface of the skull. (a) Supporting on the hypothenar eminence when working with a short instrument or in a deep operational wound, (b) touching with the fingers when working with a short instrument or in a deep operational wound, (c) touching with the little finger when working with long instruments or in a superficial operational wound, (d) complete lack of support rendering the depth of operative field arbitrary.
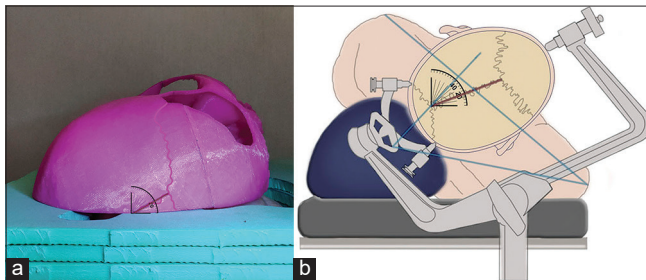

Figure 6: The base of the skull model. (a) Base angle is from 20° to 30°, (b) schematic representation of the head fixation with lateral supraorbital approach; the head inclination also varies between 20° and 30°.

Table 1: Operative approaches and distances to the operation target.

Operative approach	Depth (cm)
Retrosigmoid approach	2–4
Frontal interhemispheric approach	5–7
Expanded parietal interhemispheric approach	10–12
Occipital interhemispheric approach	5–7
Lateral supraorbital approach	4–6

By varying the approach, angle of attack, distance to operation target, and position of the hands, the trainee can practice their positioning of the instruments in the operating channel while performing manipulations.

Assessment of the 3D skull training model: a lateral supraorbital approach

Using a lateral supraorbital approach in the operating room, a roll is placed under the patient's shoulder and the head is rotated 15–30° in the direction opposite to the trepanation site. The final degree of head inclination in this position is approximately 20°. The 3D model of the lateral supraorbital approach recapitulated this skull angle [Figure 6]. In this model depth to the operation target is 6 cm. The "little finger contact" technique was used to stabilize the instruments and reduce tension in the hands because the operation was performed with long instruments in a deep wound [Figure 7d]. The operation consisted of a deep end-to-end microanastomosis of the chicken femoral artery [Figure 8]. The larger size and lack of blood flow in the chicken thigh artery when compared to a patient is a simplification and can be considered a preparatory stage before advancing to surgical training on the live animals.

Assessment of the 3D skull training model: a retrosigmoid approach

When using the retrosigmoid approach, the head is slightly inclined forward to one side and slightly rotated towards the floor, which is simulated by the angle of the slice. The distance to the operation target is 4 cm. The "little finger contact" technique was used to stabilize the instruments and reduce tension in the hands because the operation was performed with short instruments in a superficial wound [Figure 9]. The operation consisted of a deep end-to-end microanastomosis of the rat abdominal aorta [Figure 10]. The wall thickness of the rat abdominal aorta was 90 microns and the diameter was 2.1–1.9 mm. These parameters are comparable to the thickness (80 microns) and diameter (1.9–3.2 mm) of the M1 median cerebral artery.[5,22,25,31,34,36,40] This 3D skull model with a retrosigmoid approach allows trainees to
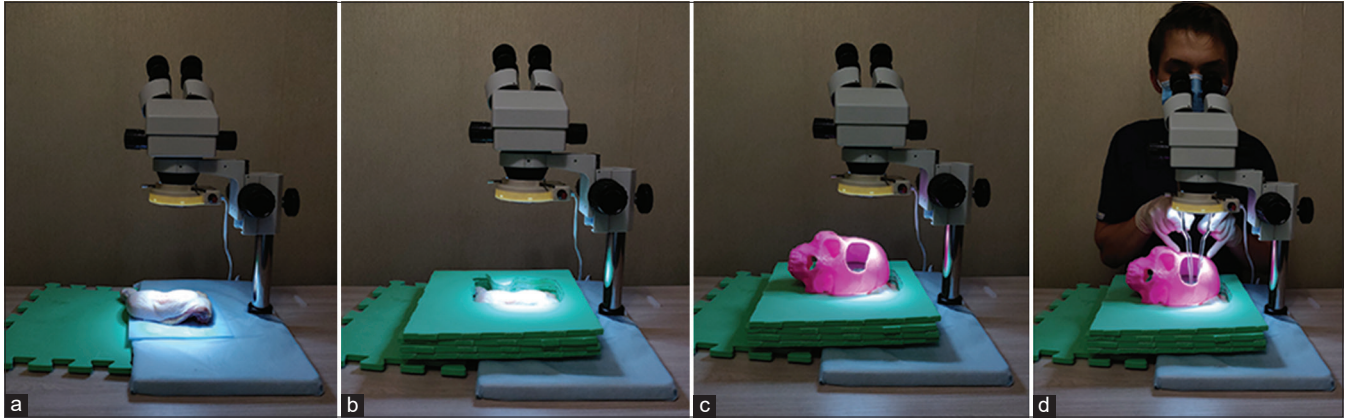
Figure 7: Use of the model through a lateral supraorbital approach when working with the chicken. (a) Placing the chicken under the microscope, (b) pad placing, (c) 3D skull model placement, (d) supporting work on the model with the little finger.
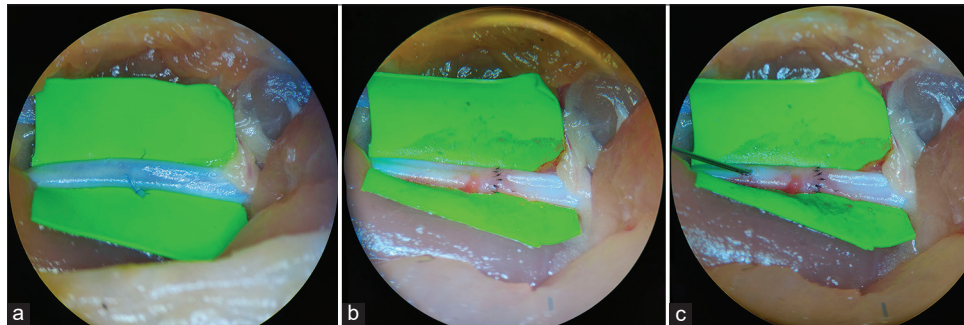

Figure 8: The femoral artery suture. (a) Use of the pad under the vessel for better visualization, (b) suturing, (c) patency test.

Figure 9: Operational support from little finger while working with rat abdominal aorta using the model through a retrosigmoid approach.

perform dissection and microanastomosis of an artery with characteristics comparable to those of human brain vessels in a deep operative field while simulating the correct angle of attack and skull stability.

DISCUSSION

The opportunity for residents and young surgeons to learn and master microsurgery skills has been significantly reduced due to the decreased volume of microsurgical cases that stemming from achievements in endovascular operations and radiosurgical therapy. Transferring the learning curve to the laboratory decreases the limitations that come with mastering practical skills in the operating room.[15] The use of 3D printed skulls is easily compatible with a staged training approach,[47] in which the training increases in complexity as the trainee becomes more comfortable. A trainee can go from a complete lack of skill to being fully prepared for solo surgeries, beginning with mastering the microscope and basic handling of microsurgical instruments and advancing to completion of superficial microvascular anastomoses.[28] The trainee can gradually hone each skill on plastic tubes, chicken arteries, and rat arteries until they are ready to proceed to an anastomosis in the deep operating field. The skull model described here allows for practice in a realistically deep operative field and width constricting instrument manipulation angles. The trainee's hands, leaning on
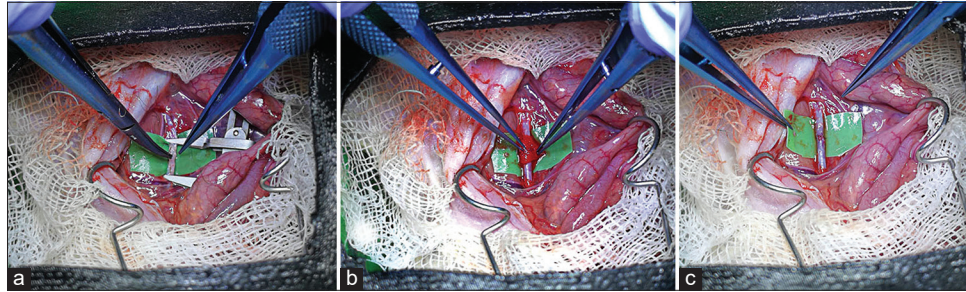
Figure 10: The formation of a deep microanastamosis. (a) Suturing, (b) performance of hemostasis, (c) completion of the operation.

the anatomical structures identical to the real ones, will experience the muscle tension felt in real operating room conditions. Beginning with chicken arteries, gradually advancing to performing a microanastomosis on a rat artery, and reducing the level of support from the hypothenar eminence to nothing, the trainee brings their skills to the point where further improvement can only be achieved in the operating room. There are certain nuances that must be considered when making an intraoperative decision that cannot be simulated in the laboratory. In addition, these 3D printed models are hollow and have no intracranial microanatomy, which significantly reduces manipulation space and increases risk. Subsequently, the trainee will eventually need to move into the operating room and begin assisting and conducting distinct stages of the operation under the close supervision of an experienced surgeon.[38] Eventually, the surgeon will master the operation and be fully prepared for solo surgery.

CONCLUSION

Deep microsurgical training is a vital component of neurosurgery. With this 3D printed skull model, training conditions can more closely resemble a real surgical environment. This model is suitable for practicing general skills of deep microsurgery, includes training variability, and allows for the improvement of microsurgical technique. The model should lead to increased confidence and efficiency of surgical procedures in the operating room, thereby minimizing risk to patients.

Declaration of patient consent

Patient's consent not required as there are no patients in this study.

Financial support and sponsorship

Nil.

Conflicts of interest

There are no conflicts of interest.

REFERENCES

1. Aderibigbe RO, Ademola S, Michael I, Olawoye O, Iyun A, Oluwatosin O. Latex glove conduit as improvised blood vessel model for microvascular anastomosis training. JPRAS Open 2020;24:15-9.
2. Atlan M, Lellouch AG, Legagneux J, Chaouat M, Masquelet AC, Letourneur D. A new synthetic model for microvascular anastomosis training? A randomized comparative study between silicone and polyvinyl alcohol gelatin tubes. J Surg Educ 2018;75:182-7.
3. Badash I, Burtt K, Solorzano CA, Carey JN. Innovations in surgery simulation: A review of past, current and future techniques. Ann Transl Med 2016;4:453.
4. Belykh E, Byvaltsev V. Off-the-job microsurgical training on dry models: Siberian experience. World Neurosurg 2014;82:20-4.
5. Belykh E, Lei T, Safavi-Abbasi S, Yagmurlu K, Almefty RO, Sun H, *et al.* Low-flow and high-flow neurosurgical bypass and anastomosis training models using human and bovine placental vessels: A histological analysis and validation study. J Neurosurg 2016;125:915-28.
6. Bjerrum F, Thomsen AS, Nayahangan LJ, Konge L. Surgical simulation: Current practices and future perspectives for technical skills training. Med Teach 2018;40:668-75.
7. Byvaltsev VA, Akshulakov SK, Polkin RA, Ochkal SV, Stepanov IA, Makhambetov YT, *et al.* Microvascular anastomosis training in neurosurgery: A review. Minim Invasive Surg 2018;2018:6130286.
8. Ceccato GH, Rassi MS, Borba LA. Microsurgical resection of a left cerebral peduncle cavernous malformation: 3-dimensional operative video. Oper Neurosurg (Hagerstown) 2020;18:E117.
9. Chae R, Sharon JD, Kournoutas I, Ovunc SS, Wang M, Abla AA, El-Sayed IH, Rubio RR. Replicating skull base anatomy with 3D technologies: A comparative study using 3D-scanned and 3D-printed models of the temporal bone. Otol Neurotol 2020;41:e392-403.
10. Chung SB, Ryu J, Chung Y, Lee SH, Choi SK. An affordable microsurgical training system for a beginning neurosurgeon: How to realize the self-training laboratory. World Neurosurg 2017;105:369-74.
11. Costa AL, Cucinotta F, Fazio A, Delia G, Galeano M, d'Alcontres FS, *et al.* Anterolateral thigh flap in a chicken model: A novel perforator training model. J Reconstr Microsurg 2019;35:485-8.
12. Council NR. Guide for the Care and Use of Laboratory

Animals. Washington, DC: National Academies Press; 2010.

13. Domingo RA, Grewal S, Tawk RG. Interhemispheric transcallosal approach for resection of choroidal arteriovenous malformation: Operative video. World Neurosurg 2020;136:73.

14. El Ahmadieh TY, Aoun SG, El Tecle NE, Nanney AD 3rd, Daou MR, Harrop J, *et al*. A didactic and hands-on module enhances resident microsurgical knowledge and technical skill. Neurosurgery 2013;73 Suppl 1:51-6.

15. Ghasemloonia A, Maddahi Y, Zareinia K, Lama S, Dort JC, Sutherland GR. Surgical skill assessment using motion quality and smoothness. J Surg Educ 2017;74:295-305.

16. Grossman LB, Komatsu DE, Badalamente MA, Braunstein AM, Hurst LC. Microsurgical simulation exercise for surgical training. J Surg Educ 2016;73:116-20.

17. Hendricks BK, Spetzler RF. Far-lateral approach for medullary cavernous malformation: 2-dimensional operative video. Oper Neurosurg (Hagerstown) 2020;18:E74-5.

18. Hendricks BK, Spetzler RF. Microsurgical resection of brainstem arteriovenous malformation: 2-dimensional operative video. Oper Neurosurg (Hagerstown) 2020;18:E38.

19. Heskin L, Simms C, Holland J, Traynor O, Galvin R. A systematic review of the educational effectiveness of simulation used in open surgery. Simul Healthc 2019;14:51-8.

20. Jeon HJ, Kim SY, Park KY, Lee JW, Huh SK. Ideal clipping methods for unruptured middle cerebral artery bifurcation aneurysms based on aneurysmal neck classification. Neurosurg Rev 2016;39:215-24.

21. Kang BY, Jeon BJ, Lee KT, Mun GH. Comprehensive analysis of chicken vessels as microvascular anastomosis training model. Arch Plast Surg 2017;44:12-8.

22. Kim IS, Jo WM. Effects of a proteasome inhibitor on cardiomyocytes in a pressure-overload hypertrophy rat model: An animal study. Korean J Thorac Cardiovasc Surg 2017;50:144-52.

23. Lawton MT, Lang MJ. The future of open vascular neurosurgery: Perspectives on cavernous malformations, AVMs, and bypasses for complex aneurysms. J Neurosurg 2019;130:1409-25.

24. Lee BS, Witek AM, Moore NZ, Bain MD. Treatment of an anterior inferior cerebellar artery aneurysm with microsurgical trapping and *in situ* posterior inferior cerebellar artery to anterior inferior cerebellar artery bypass: Case report. Oper Neurosurg (Hagerstown) 2018;15:418-24.

25. Lin JS, Wang CJ, Li WT. Photodynamic therapy of balloon-injured rat carotid arteries using indocyanine green. Lasers Med Sci 2018;33:1123-30.

26. Lopez-Gonzalez MA, Sharafeddin F, Eastin TM, Gospodarev V, Jaeger A. Microsurgical technique for basilar apex aneurysm clipping: Two-dimensional video. World Neurosurg 2019;126:467.

27. Madhugiri VS, Teo MK, Westbroek EM, Chang SD, Marks MP, Do HM, *et al*. Multimodal management of arteriovenous malformations of the basal ganglia and thalamus: Factors affecting obliteration and outcome. J Neurosurg 2018;131:410-9.

28. Malik MM, Hachach-Haram N, Tahir M, Al-Musabi M, Masud D, Mohanna PN. Acquisition of basic microsurgery skills using home-based simulation training: A randomised control study. J Plast Reconstr Aesthet Surg 2017;70:478-86.

29. Mikami T, Suzuki H, Ukai R, Komatsu K, Kimura Y, Akiyama Y, *et al*. Surgical anatomy of rats for the training of microvascular anastomosis. World Neurosurg 2018;120:e1310-e8.

30. Olijnyk LD, Patel K, Brandão MR, de Morais AN, de Carvalho RF, Severino AG, *et al*. The role of low-cost microsurgical training models and experience with exercises based on a bovine heart. World Neurosurg 2019;130:59-64.

31. Pahk K, Joung C, Jung SM, Song HY, Park JY, Byun JW, *et al*. Visualization of synthetic vascular smooth muscle cells in atherosclerotic carotid rat arteries by F-18 FDG PET. Sci Rep 2017;7:6989.

32. Pitskhelauri D, Konovalov A, Kudieva E, Bykanov A, Pronin I, Eliseeva N, *et al*. Burr hole microsurgery for intracranial tumors and mesial temporal lobe epilepsy: Results of 200 consecutive operations. World Neurosurg 2019;126:e1257-67.

33. Ramachandran S, Ghanem AM, Myers SR. Assessment of microsurgery competency-where are we now? Microsurgery 2013;33:406-15.

34. Ren XS, Ling L, Zhou B, Han Y, Zhou YB, Chen Q, *et al*. Silencing salusin-β attenuates cardiovascular remodeling and hypertension in spontaneously hypertensive rats. Sci Rep 2017;7:43259.

35. Reznick RK, MacRae H. Teaching surgical skills-changes in the wind. N Engl J Med 2006;355:2664-9.

36. Rubies C, Dantas AP, Batlle M, Torres M, Farre R, Sangüesa G, *et al*. Aortic remodelling induced by obstructive apneas is normalized with mesenchymal stem cells infusion. Sci Rep 2019;9:11443.

37. Shen Z, Yao Y, Xie Y, Guo C, Shang X, Dong X, *et al*. The process of 3D printed skull models for anatomy education. Comput Assist Surg (Abingdon) 2019;24:121-30.

38. Shiu B, Petkovic D, Levine WN, Ahmad CS. Maximizing surgical skills during fellowship training. J Am Acad Orthop Surg 2017;25:421-6.

39. Steinberg JA, Rennert RC, Levy M, Khalessi AA. A practical cadaveric model for intracranial bypass training. World Neurosurg 2019;121:e576-83.

40. Tan B, Gurdita A, Choh V, Joos KM, Prasad R, Bizheva K. Morphological and functional changes in the rat retina associated with 2 months of intermittent moderate intraocular pressure elevation. Sci Rep 2018;8:7727.

41. Wainberg RC, da Costa MD, Hernández YA, Caramanti RL, Filho CA, Palmiero H, *et al*. Microsurgical clipping of ruptured distal posterior inferior cerebellar artery aneurysm: 3-dimensional operative video. Oper Neurosurg (Hagerstown) 2019;16:E48-9.

42. Wolfswinkel EM, Landau MJ, Ravina K, Kokot NC, Russin JJ, Carey JN. EC-IC bypass for cerebral revascularization following skull base tumor resection: Current practices and innovations. J Surg Oncol 2018;118:815-25.

43. Yasuda T, Maki Y, Ishibashi R, Kurosaki Y, Chin M, Yamagata S. Distal posterior inferior cerebellar artery aneurysm with cerebellar arteriovenous malformation treated by open surgery: A case report. Chin Neurosurg J 2019;5:15.

44. Yin X, Ye G, Lu J, Wang L, Qi P, Wang H, *et al*. A novel rat model for comprehensive microvascular training of end-to-end, end-to-side, and side-to-side anastomoses. J Reconstr Microsurg 2019;35:499-504.

45. Zada G, Bakhsheshian J, Pham M, Minneti M, Christian E, Winer J, *et al.* Development of a perfusion-based cadaveric simulation model integrated into neurosurgical training: Feasibility based on reconstitution of vascular and cerebrospinal fluid systems. Oper Neurosurg (Hagerstown) 2018;14:72-80.
46. Zenonos GA, Sur S, Nuñez M, Fernandes-Cabral DT, Morcos JJ. Far lateral approach for resection of lower pontine cavernous malformation. Neurosurg Focus 2019;1:V27.
47. Zhou S, Li E, He J, Weng G, Yuan H, Hou J. Staged microvascular anastomosis training program for novices: Transplantation of both kidneys from one rat donor. Chin Med J (Engl) 2014;127:712-7.